The Functional Roles of the Amygdala and Prefrontal Cortex in Processing Uncertainty

Oriel FeldmanHall[1], Paul Glimcher[2], Augustus L. Baker[2], NYU PROSPEC Collaboration*, and Elizabeth A. Phelps[2,3]

Abstract

■ Decisions under uncertainty distinguish between those made under risk (known probabilities) and those made under ambiguity (unknown probabilities). Despite widespread interest in decisions under uncertainty and the successful documentation that these distinct psychological constructs profoundly—and differentially—impact behavior, research has not been able to systematically converge on which brain regions are functionally involved in processing risk and ambiguity. We merge a lesion approach with computational modeling and simultaneous measurement of the arousal response to investigate the impact the medial prefrontal cortex (mPFC), lateral prefrontal cortex (lPFC), and amygdala have on decisions under uncertainty. Results reveal that the lPFC acts as a unitary system for processing uncertainty: Lesions to this region disrupted the relationship between arousal and choice, broadly increasing both risk and ambiguity seeking. In contrast, the mPFC and amygdala appeared to play no role in processing risk, and the mPFC only had a tenuous relationship with ambiguous uncertainty. Together, these findings reveal that only the lPFC plays a global role in processing the highly aversive nature of uncertainty. ■

INTRODUCTION

Choosing which route to take to work, entrée to select on the menu, or friend to entrust with a secret are all decisions made under uncertainty. These decisions, which are part and parcel of everyday human life, can be characterized as either those made under risk (known probabilities) or those made under ambiguity (unknown probabilities; Knight, 1921). The distinction between these two types of uncertainty illustrates that humans have a strong aversion to ambiguous uncertainty compared with risky uncertainty—even when risky and ambiguous decisions share the same probabilistic outcomes (Ellsberg, 1961). Recent work exploring the underlying mechanisms motivating aversion to ambiguity found that affect, indexed through arousal, appears to play a fundamental, and perhaps specific, role in biasing the representation of value under ambiguity (FeldmanHall, Glimcher, Baker, & Phelps, 2016). Evidence from the imaging literature corroborates this, demonstrating that neural systems intimately linked with processing affect and arousal are critically involved when humans make decisions under uncertainty (Levy, Snell, Nelson, Rustichini, & Glimcher, 2010; Huettel, Stowe, Gordon, Warner, & Platt, 2006; Critchley, Mathias, & Dolan, 2001). However, despite the active and interdisciplinary nature of this research topic, there is little consensus about which brain regions are essential for processing decisions of risk versus those made under ambiguity. Accordingly, precisely quantifying the role of affect, and identifying the associated neural regions necessary when making decisions under uncertainty, has remained elusive. To do this, we leverage computational models with physiological methodologies in patients with brain lesions to test the causal and putatively selective role affect plays in processing and biasing decisions under ambiguity, compared with those under risk.

The past two decades have been very productive in identifying the network of brain regions involved in processing uncertainty. Early work found that lesions to the medial prefrontal cortex (mPFC) appeared to have a profound impact on detecting uncertainty, which hindered adaptive decision-making (Bechara, 2004; Bechara, Damasio, & Damasio, 2000). This research was seminal in demonstrating how key brain regions involved in affect—indexed through the body's arousal response—are necessary for successfully responding to uncertainty. This work, however, failed to differentiate between the psychological constructs of risk and ambiguity, leaving the specific role of the mPFC and putative engagement of the affective system in guiding such decisions unclear. In contrast, subsequent studies employing imaging methods and formal decision models have successfully differentiated decisions of risk from ambiguity, finding increased BOLD activation in a suite of brain regions, including the mPFC (and OFC), amygdala, lateral prefrontal

[1]Brown University, Providence, RI, [2]New York University, [3]Nathan Kline Institute, Orangeburg, NY
*The authors of the NYU PROSPEC Collaboration are listed in the Acknowledgments.

Journal of Cognitive Neuroscience 31:11, pp. 1742–1754
https://doi.org/10.1162/jocn_a_01443

cortex (lPFC), and cingulate (Levy et al., 2010; Huettel et al., 2006; Critchley et al., 2001).

Despite the behavioral evidence that these are likely distinct psychological constructs (Tymula, Rosenberg Belmaker, Ruderman, Glimcher, & Levy, 2013), the literature has not been able to systematically converge on which brain regions are necessary for processing risk compared with ambiguity, and vice versa. For example, some work exclusively examining risk found a key role for the OFC, cingulate, and lPFC in modulating risky choices (Levy et al., 2010; Critchley et al., 2001), whereas a later study reported a different pattern of results, observing that risky decisions engaged the caudate, while ambiguous decisions more consistently elicited BOLD activity in the OFC and amygdala (Levy et al., 2010; Hsu, Bhatt, Adolphs, Tranel, & Camerer, 2005). A flurry of work across many laboratories followed suit, revealing more inconsistent evidence about whether the OFC and amygdala are more involved in decisions under ambiguity compared with risk and whether regions such as the lPFC are more integral for processing risk relative to ambiguity. This inconsistent evidence is often leveraged to support two competing theoretical accounts: a dissociable neural system where different neural networks index risk and ambiguity (Krain, Wilson, Arbuckle, Castellanos, & Milham, 2006) and a common neural system supporting both types of uncertainty (Hsu et al., 2005). More than a decade later, there is little resolution.

Although the vast majority of research has employed imaging methods to investigate the neural mechanisms supporting risk and ambiguity, the brain's BOLD signal cannot capture causal relationships, leaving the necessity of specific brain regions in question. The one instance in which a lesion method was used also paints a conflicting story: Hsu and colleagues found that ambiguous (compared with risky) decisions correlated with increased BOLD activity in the lateral OFC (Hsu et al., 2005). However, when examining a small sample of patients with damage to this region, the authors reported impaired behavioral patterns for both risky and ambiguous choices. Given the contradictory evidence on all levels, pressing questions remain. Does a unified integrated neural network process both types of uncertainty, or are there two separate and dissociable systems for processing risk and ambiguity? If there are indeed two systems, is there a quantifiably unique affective signal that is sensitive to the more aversive nature of decisions made under ambiguity compared with those made under risk?

We merge a lesion approach with computational modeling to investigate the relationships between brain regions and their impact on decisions of risk and ambiguity. By documenting how specific brain lesions relate to observable behavioral deficits, we can gain a deeper understanding of the contributions for many of the brain areas implicated in processing decisions of uncertainty. Accordingly, using a well-vetted gambling task (Figure 1)

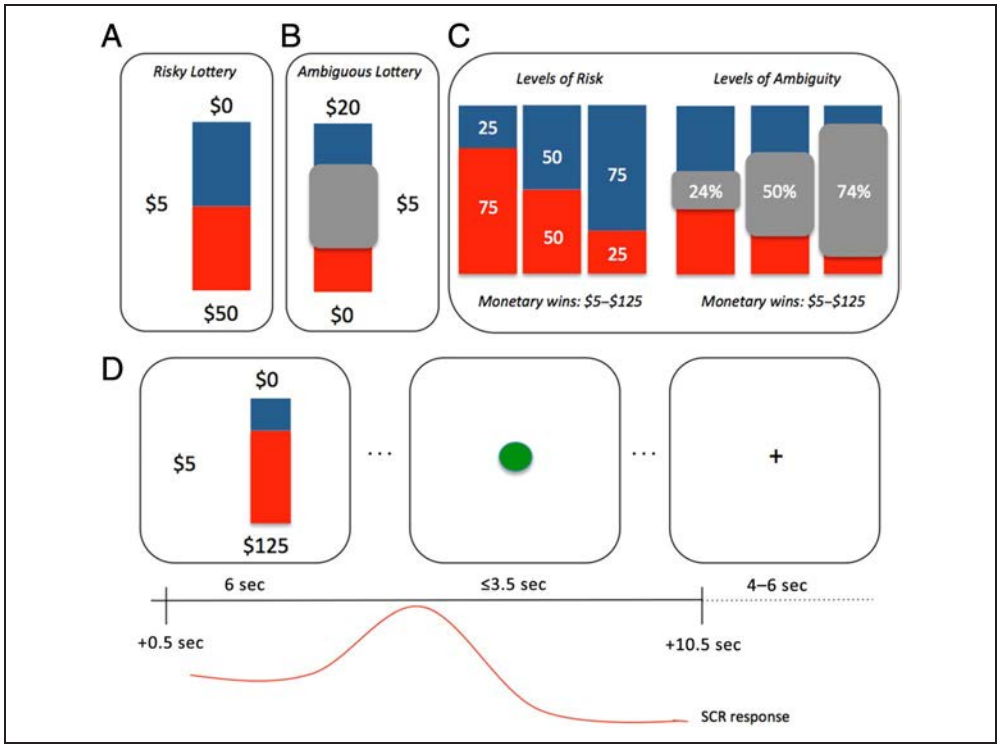

Figure 1. Experimental design. Participants completed a standard computerized lottery task where each lottery depicted a stack of 100 red and blue poker chips that corresponded to actual payout bags in the testing laboratory. On each trial, participants could choose between receiving $5 for sure versus taking a gamble. (A) An example of a risky trial that contained 50/50 odds of winning $50 (i.e., 50% risky gamble). (B) An example of an ambiguous trial where 50% of the chips are occluded (i.e., 50% ambiguity). In this case, the participant could gamble for $20 or take the sure $5. (C) Risky trials were always presented as 25% (high risk), 50%, or 75% (low risk) probability of winning. During ambiguity trials, the probabilities were occluded to varying degrees (three levels were used) ranging from 24% to 74%. The monetary wins were always counterbalanced between red and blue chips and were matched across risky and ambiguous trials. (D) Each trial consisted of a fixed lottery presentation for 6 sec. Once a green dot appeared, the participant could key in their response to indicate playing the lottery or taking the safe bet. SCR was recorded for 10 sec starting 0.5 sec after the lottery presentation onset.

known to dissociate risk and ambiguity (Grubb, Tymula, Gilaie-Dotan, Glimcher, & Levy, 2016; Tymula et al., 2012, 2013; Levy et al., 2010), we implemented a formal model that captures individuals' risk and ambiguity attitudes (Gilboa & Schmeidler, 1989) to interrogate the role of the mPFC, lPFC, and amygdala and their relative contributions to risk and ambiguity intolerance. This is done while simultaneously measuring skin conductance responses (SCRs), which allows us to collect converging evidence on the specific effects of whether the integration of arousal during the decision process is impaired. Taken together, this approach permits a systematic investigation of whether specific brain regions systematically bias the computation of value of choice depending on whether the decision was purely risky or ambiguous.

METHODS

Participants

Healthy Controls

We recruited 44 healthy controls (HCs), matched in age, gender, and education to our patient group (see below). Sample size was determined from past work using the same task (FeldmanHall et al., 2016). Four participants were not included in the analysis for the following reasons: One participant was excluded for failing to understand the task during debriefing and because his or her SCR and behavioral data were subsequently never scored, and an additional three participants were not included because of technical difficulties or for failing to exhibit any SCR during the initial test phase, which required participants to hold their breath (see section on SCR for more details). The final sample, which was recruited from the New York University Patient Registry for the Study of Perception, Emotion and Cognition, included 40 participants (23 women; mean age = 33.5 years, SD = 11.5).

Patients

Thirty-three patients with brain lesions because of stroke, tumor resection, head injury, and surgery for epilepsy (Table 1) were recruited from the Patient Registry for the Study of Perception, Emotion and Cognition (15 women; mean age = 40.2 years, SD = 11.1). Using MRIcron and FSLView software, lesion masks for each patient were created by a clinical neuropsychologist before data collection, which allowed us to classify patients into different lesion groups reflecting the primary location of the lesion, resulting in the final grouping: lPFC patients, n = 8; mPFC patients, n = 9; and medial temporal lobe (MTL; where the maximum overlap was in the amygdala) patients, n = 16. The clinical neuropsychologist also carried out a clinical interview and a comprehensive neuropsychological examination to evaluate cognitive abilities and current social functioning before data collection. Each patient's medical records and high-resolution T1 magnetization prepared rapid gradient echo (MP-RAGE) scans were evaluated and used to determine if there was evidence of diffuse atrophy. If there was, patients were excluded from recruitment. Evidence of (1) global cognitive dysfunction on a standard measure of intelligence (Wechsler Adult Intelligence Scale–Fourth Edition: index scores below the standard score of 70; Wechsler, Coalson, & Raiford, 2008), (2) a history of developmental/learning disorders, (3) intellectual disability (full-scale IQ < standard score of 70), (4) severe psychiatric illness, or (5) complicating neurologic conditions other than those related to the brain lesions were also used to exclude patients during recruitment (Table 2).

Creation of Lesion Masks

Postsurgical scans were obtained using 1.5- or 3-T Siemens full-body MR scanners from the NYU Radiology Department. Image acquisitions included a conventional three-plane localizer and two T1-weighted gradient-echo sequence volumes. High-resolution T1 MP-RAGE sequences from each patient were normalized to Montreal Neurological Institute standard space. Using MRIcron, a mask was drawn over the lesion and any craniotomy defect, where masked voxels were assigned a weight of 0, elsewise 1—indicating the presence of intact tissue. Two frontal patients had bilateral damage. In a few cases, the damage was highly extensive (such that seven to eight Brodmann's areas were, at least in part, damaged), which resulted in large swaths of the frontal region being removed. However, for most of the frontal patients, the lesions were more constrained such that only a few Brodmann's areas were affected. All MTL patients had unilateral lesions, and many had damage to both the amygdala and hippocampal structures. In most cases, the damage encompassed the anterior hippocampus; however, the posterior hippocampus was preserved. In very few patients was the entire hippocampus lesioned. About a third of the MTL patients also had some damage to the anterior temporal pole.

In the rare circumstances when we were unable to obtain a postoperative T1 MP-RAGE (one patient was highly claustrophobic), we used the patient's preoperative MRI to determine the tumor location and estimate the location of the postoperative lesion. The clinical neuropsychologist, in conjunction with a trained MRI physicist at the NYU Center for Brain Imaging, then reconstructed a patient's T1 MRI scan on a 3-T Siemens Allegra head-only MR scanner.

Creation of ROI Masks

ROI masks were constructed with MarsBar toolbox (Brett, Anton, Valabregue, & Poline, 2002) by combining corresponding structures from the Harvard-Oxford Maximum Probability Atlases (Fischl et al., 2004). Our two ROIs localized to the PFC consisted of the mPFC

Table 1. Lesion Descriptions

Patient	*Group*	*Lesion Location*	*Etiology*	*Handedness*	*Lesion Volume (Percent Damage)*
3	MTL	R	Medial temporal sclerosis, epilepsy	R	3.12
5	MTL	L	Medial temporal sclerosis, epilepsy	R	3.99
10	MTL	R	Dysembryoplastic neuroepithelial tumor in anterior mesial temporal lobe	L	2.80
14	MTL	L	Medial temporal sclerosis, epilepsy	R	1.63
27	MTL	R	Epilepsy	R	2.32
31	MTL	R	Epilepsy	R	2.05
53	MTL	L	Epilepsy	R	3.87
56	MTL	R	Epilepsy	R	5.03
58	MTL	R	Epilepsy	R	3.91
80	MTL	R	Epilepsy	R	3.02
83	MTL	L	Epilepsy	R	1.77
99	MTL	L	Epilepsy	R	2.07
153	MTL	R	Epilepsy	R	4.61
178	MTL	L	Epilepsy	L	2.60
182	MTL	L	Epilepsy	R	1.81
184	MTL	L	Epilepsy	R	2.51
41	lPFC	L	Glial tumor	R	2.12
45	lPFC	L	Epilepsy and hemorrhage	L	Not available
52	lPFC	L	Oligodendroglioma (low-grade)	R	1.78
81	lPFC	R	Low-grade glioma	R	4.52
95	lPFC	Bilateral	Meningioma	R	5.69
100	lPFC	R	Focal cortical dysplasia	R	5.88
105	lPFC	L	Cavernoma	R	0.10
108	lPFC	L	Hamartoma with balloon cells	R	1.15
34	mPFC	L	Oligodendroglioma and epilepsy	R	5.01
35	mPFC	L	Oligodendroglioma (low-grade)	R	1.46
36	mPFC	L	Neoplasm (glioma)	R	3.54
46	mPFC	R	Epilepsy	R	9.20
122	mPFC	L	Epilepsy	R	7.96
123	mPFC	L	Cavernous angioma resection	R	Not available
133	mPFC	R	Malformation of cortical development in inferior frontal lobe and frontal basal cavernoma	R	2.56
156	mPFC	R	Glioma surrounding right eye orbit	R	Not available
186	mPFC	Bilateral	Traumatic brain injury	Mixed (R > L)	6.72

Lesion volume is indexed by the percentage of damaged voxels across the whole-brain mask. L = left; R = right.

Table 2. Group Demographics

Group	*Sex*	*Age (SD)*	*Years of Education*	*FSIQ*	*VCI*	*PRI*	*WMI*	*PSI*
mPFC	4 female	41.7 (12.4)	16.3	104.3	108.9	104.4	97.6	99.8
lPFC	1 female	41.5 (15.1)	13.9	101.9	110.0	98.9	100.9	94.0
Amygdala	10 female	37.6 (8.4)	15.7	105.9	106.6	103.9	104.6	104.2

Neuropsychological scores of patients after resection for the Wechsler Adult Intelligence Scale: full-scale IQ (FSIQ), verbal comprehension index (VCI), perceptual reasoning index (PRI), working memory index (WMI), and processing speed index (PSI).

and lPFC (see Supplementary Material[1] for images of the ROIs; Figure S6). The mPFC ROI consisted of the frontal pole, frontal medial cortex, paracingulate gyrus, and subcallosal cortex and was constrained by rectangular prism $x = [-14, 14]$, $y = [10, 80]$, $z = [-35, 0]$. The lPFC ROI consisted of the inferior frontal gyrus and middle frontal gyrus and was constrained by bilateral rectangular prism $x = [-60, -30$ (L); $30, 60$ (R)$]$, $y = [20, 70]$, $z = [5, 55]$. Five participants had damage to both lPFC and mPFC, but in each case, patients had more damage to either the lPFC ($n = 3$) or the mPFC ($n = 2$), using the parameters defined by the ROI mask (see Table 1). Finally, amygdala ROIs were created using the Harvard-Oxford Subcortical Atlas thresholded at 25% probability.

ROI Analysis

To determine the extent of damage and its relative contribution to risk and ambiguity preferences, we first estimated the proportion of each individual's damage within each ROI mask. For example, a patient with damage to 10% of the lPFC mask would receive a value of 0.10. Some patients, especially those with frontal damage, exhibited damage to both the medial and lateral portions of PFC (two in total). In these cases, patients with greater damage in one ROI (e.g., 33% damage to the mPFC and 10% damage to the lPFC) were categorized according to the ROI with the greatest damage. These percentages were used as independent variables at the participant level in linear regressions (Tables 3 and 4).

Task

To characterize the relevant engagement of the brain regions known to be involved in processing affect, as well as the possible role of arousal in guiding risky and ambiguous decisions, participants performed a well-vetted task (FeldmanHall et al., 2016; Grubb et al., 2016; Tymula et al., 2012; Levy et al., 2010) composed of gambles with known probabilities (risky trials, Figure 1A) and unknown probabilities (ambiguous trials, Figure 1B). On each of the 62 trials, participants had the option to choose the safe option with a sure payout of $5 or to take the gamble (payouts between $5 and $125), where each gamble had varying degrees of monetary value, and risk or ambiguity (Figure 1C). Each lottery was either risky or ambiguous, allowing us to assess an individual's sensitivity to known risk and unknown ambiguous monetary choices. The parameters of the lottery were varied in random order, such that the magnitude of the potential win (money) and the probability of winning (risk and ambiguity levels) could independently influence participants' choices. Figure 1A depicts a risky trial where a participant could choose between $5 for sure (available on every trial) or a lottery with a 50% chance of winning $50 or nothing ($0). All lotteries are presented by a bag composed of blue and

Table 3. Model-Free Results: Effect of Brain Damage on Risky Gambles: All Patient Groups

Dependent Variable	*Coefficient* (β)	β *Estimate (SE)*	*t Value*	*p Value*
Risky Choice				
	Intercept	0.08 (0.06)	−1.29	.19
	mPFC percent damage	−0.38 (0.98)	−0.39	.69
	lPFC percent damage	3.0 (1.3)	2.2	.02*
	Amygdala percent damage	0.75 (0.63)	1.19	.23
	Total percent damage	−8.18 (6.0)	−1.36	.17

$\text{Risky Choices}_{i,t} = \beta_0 + \beta_1$ mPFC Percent $\text{Damage}_i + \beta_2$ lPFC Percent $\text{Damage}_i + \beta_3$ Amygdala Percent $\text{Damage}_i + \beta_4$ Total Percent Damage_i. Where Choice is indexed by participant and trial and Percent Damage is indexed by participant and accounts for the number of voxels damaged in each ROI (see methods for ROI creation).

*$p < .05$.

Table 4. Model-Free Results: Effect of Brain Damage on Ambiguous Gambles—All Patient Groups

Dependent Variable	*Coefficient* (β)	β *Estimate (SE)*	*t Value*	*p Value*
Ambiguous Choice				
	Intercept	−0.17 (0.10)	−1.44	.15
	mPFC percent damage	1.02 (1.51)	0.67	.49
	lPFC percent damage	3.58 (1.85)	1.93	.054*
	Amygdala percent damage	0.87 (1.07)	0.81	.41
	Total percent damage	−16.3 (10.37)	−1.56	.11

Ambiguous Choices$_{i,t}$ = β_0 + β_1 mPFC Percent Damage$_i$ + β_2 lPFC Percent Damage$_i$ + β_3 Amygdala Percent Damage$_i$ + β_4 Total Percent Damage$_i$. Where Choice is indexed by participant and trial and Percent Damage is indexed by participant and accounts for the number of voxels damaged in each ROI (see methods for ROI creation).

*$p < .1$.

red chips. In this particular case, there are 50 blue chips and 50 red chips and the winning amount happens to be associated with the red chips. Thus, if the participant draws a red chip, he or she wins the lottery. For these risky trials, outcome probabilities were fully stated with varying winning probabilities of 25%, 50%, and 75%.

During ambiguous trials, the probabilities were occluded to varying degrees. For example, participants could face either a sure payout of $5 or a lottery paying $20 (associated, e.g., with the red chips) or $0 (associated with the blue chips), with a gray occluder covering 50% of the poker chips (50% ambiguity). Thus, the participant knows there are at least 25 red and 25 blue chips, but the remaining 50 can be any combination of red and blue. Depending on the participant's ambiguity intolerance, one could perceive the odds of winning $20 to be anywhere from 24% to 74%. Occluder size ranged from 24% (low ambiguity) to 50% (medium ambiguity) to 74% (high ambiguity), where increasing occluder size reduces information about the contents of the bag, raising the level of ambiguity (Figure 1C). The lotteries for both types of risk corresponded to actual bags filled with red and blue chips placed in the testing laboratory and that were used to pay participants. For each participant, color associated with winning the monetary reward was counterbalanced, as was the side the lottery option was presented. Although aversion to uncertainty is greater in the loss than gain domain, our prior work illustrates that, regardless of the domain, these are stable preferences that are consistently held over time; thus, we only examined risk and ambiguity within the gain domain (Tymula et al., 2013).

Lotteries were presented for a fixed 6 sec, at which time a green button appeared cuing the participant to key in their response. Participants had up to 3.5 sec to make a response. Once a response was recorded, participants viewed a schematic of which button they pressed, providing visual feedback of the choice they made (presented for 1 sec). The intertrial interval was a fixation cross presented for a jittered 4–6 sec, which allowed us to effectively measure trial-by-trial SCRs.

Payment

Past research, including work from our own laboratory, indicates that people behave differently when their choices are hypothetical (FeldmanHall et al., 2012; Holt & Laury, 2002). Accordingly, participants' choices were consequential, with one trial randomly selected for payout. Thus, all participants understood that their decision on that trial would result in real monetary consequence. To pay out the participants, experimenters created a number of paper bags with lottery images that corresponded to those used in the task. The bags were filled with a number of blue and red poker chips proportional to the outcome probability stated by the lottery display. After completion of the task, each participant drew a numbered poker chip from a separate paper bag to select a random trial for payment. If on the selected trial the participant chose to gamble, the lottery depicted in the trial was played by drawing a chip from the corresponding paper bag. If the participant drew a chip corresponding with winning the lottery, they received a bonus payment equal to the value of the gamble (between $5 and $125); if they drew a losing chip, they were not able to make additional money and were compensated $15 for participating in the study. If on the selected trial the participant chose the sure outcome, they received an additional $5 in compensation.

To ensure that participants understood the task and payout structure, at the end of the computer-presented instructions and before the 10 practice trials, the experimenter always said: "So I want to explain how payment works. As you can see, we have multiple bags lined up. Each bag has a picture that matches each lottery image used in the experiment. The outcome probabilities are stated here (point to bags). In other words, these pictures of the probabilities correspond to the options you

will see during the experiment. Please make sure you understand this, as we will use these bags later to pay you out for one randomly selected lottery. To reiterate, you will be paid out based on your choices, and these bags will be used later to play randomly chosen trials for payoff. After the experiment, you will be allowed to look inside the bags to see that they match the stated probability or ambiguity level pictured here."

SCR Collection

To measure the body's arousal response, SCR was recorded while participants viewed the lottery and made their decision (10-sec window, Figure 1D). Because raw SCRs were positively skewed, participants' SCRs were normalized by taking the square root of each base-to-peak score. Participants performed the task in an experiment room equipped with an MP-150 BIOPAC system used to record SCRs. Before the task, participants read through the instructions and practiced the task for 10 trials. The experimenter then attached the BIOPAC sensors to participants' left palm and instructed them to keep their arm as still as possible for the duration of the study to collect SCRs. The experimenter always performed two tests to ensure that SCR responses could be collected. After allowing a baseline SCR to develop, the experimenter instructed the participants to take a deep breath and hold it for 3 sec to determine if adequate SCRs could be produced. For the second test, the experimenter asked participants to purse their lips and blow air as if they were inflating a balloon, but without releasing their breath. If one or both tests produced an adequate SCR response, the experimenter continued with the experiment; otherwise, the participant was compensated $15 and dismissed without completing the task. The experimenter remained in the room with the participants for the duration of the study to monitor their SCR recording and to transition them from Blocks 1 to 2 of the task.

SCRs were recorded and analyzed using AcqKnowledge (Version 3.7.3, BIOPAC Systems Inc.). The data were collected at 200 samples per second using a low-pass digital filter with a 25-Hz cutoff frequency and a smoothing factor of 10 samples. SCRs were considered related to the choice if the base-to-peak response (i.e., $SCR_{max} - SCR_{min}$) was within the established window of 0.5 sec after the onset of the stimulus to 0.5 sec after the offset of the stimulus (10.5 sec in total; see Figure 1D). Responses starting before 0.5 sec after the onset are unable to be considered elicited by the stimulus and were thus not analyzed (Dawson, Schell, & Filion, 2007).

Threshold response criterion was set at 0.02 μV or greater, and responses that failed to meet this criterion were scored as 0 (Dawson et al., 2007). Because raw SCRs follow a skewed distribution, SCRs were normalized by taking the square root of each score as commonly done in studies that measure electrodermal activity (Dawson et al., 2007), which allows for SCR data to be analyzed using parametric tests. For analyses that required SCRs to be compared between HCs and lesion populations, we transformed SCRs first into z scores and then into t scores by using the mean and standard deviation of each group (Braithwaite & Watson, 2015). The advantage of this approach is that it allows a direct comparison between groups, without relying on the assumption about maximum SCR responding (Boucsein, 1992).

Modeling of Risk and Ambiguity Attitudes

The gambling task we employed allows us to explicitly explore the relationship between affective arousal and gambling rates by modeling the subjective value of risk and ambiguity for each option under consideration and the amount of money that can be gained. In our past work, we found that Gilboa and Schmeidler's maxmin expected utility model provides a simple and useful model anchoring parameters for best- and worst-case scenarios (Gilboa & Schmeidler, 1989), where one parameter indicates risk sensitivity (α) and the second parameter indicates ambiguity sensitivity (β). This utility function takes into account the effect of ambiguity on perceived winning probability:

$$SV(p, A, \nu) = \left(p - \beta * \frac{A}{2}\right) * \nu^{\alpha}$$

where, for each trial, subjective value is calculated as a function of the lottery's objective winning probability (p), level of ambiguity (A), and monetary value (ν), accounting for each individual's risk (α) and ambiguity (β) attitudes, which are obtained from the behavioral fit of the model (see below). An $\alpha > 1$ indicates that a person is risk seeking and thus more likely to gamble on risky trials, whereas an $\alpha < 1$ indicates that a person is risk averse and less likely to gamble on risky trials ($\alpha = 1$ indicates a risk-neutral individual). A $\beta > 0$ indicates that a person is ambiguity averse and thus less likely to gamble on ambiguous trials, whereas a $\beta < 0$ indicates that a person is ambiguity seeking and thus more likely to gamble during ambiguous lotteries. These estimates have opposite polarities, reflecting participants' attitudes toward risk and ambiguity based on their decisions during the task. Classically used by Holt and Laury (2002), as well as in prior work from our laboratory (FeldmanHall et al., 2016; Levy et al., 2010), these attitudes were derived by fitting choice data using the maximum likelihood with the following probabilistic choice function:

$$P(\text{choose lottery}) = \frac{1}{1 + e^{\gamma(SV_F - SV_V)}}$$

where SV_F and SV_V are the subjective values of the fixed and variable options, respectively, and γ is the slope of the logistic function, which is a participant-specific parameter. This utility function captures the relative value

a participant places on ambiguous versus risky lotteries, allowing us to decompose the subjective value of each lottery and explore its discrete relationship with the arousal response. All analyses and results employing the model-based approach can be found in the supplement.

Model-Free Approach

We also examined the impact of brain damage on choice by looking at raw decisions to gamble or take the safe bet. To do this, we employed a trial-by-trial hierarchal regression framework. For example, to examine the lesion–gambling relationship, we modeled the binary choice to gamble or take the safe option as a function of the amount of damage to each lPFC, mPFC, and amygdala ROIs, while also controlling for overall damage. We also used a similar approach to explore the arousal–gambling relationship; we modeled the binary choice to gamble or take the safe option as a function of SCR under each type of uncertainty—for each level of risk and ambiguity. For these regressions, we used the fitglme function in MATLAB, such that the decision data were modeled with a binomial distribution and a Logit link function. We report maximal models (random and fixed effects are included in regressions) for all analyses (Barr, Levy, Scheepers, & Tily, 2013).

RESULTS

Choices Under Uncertainty

To examine how lesions to the lPFC, mPFC, and amygdala might affect decisions under uncertainty, we took the number of trials on which a participant selected the risky or ambiguous lottery and used this as an index of their willingness to engage in risky or ambiguous decision-making. We ran a hierarchal logistic regression, interrogating choice (rates of selecting risky and ambiguous lotteries) as a function of the extent of damage to a given ROI (i.e., the number of voxels damaged in each patient within a given ROI mask). One advantage of this approach is that not only is the raw gambling rate of each participant accounted for, but the regression additionally accounts for the percent damage to predetermined ROIs. For an alternative approach that uses a parametric model-based approach (i.e., Gilboa and Schmeidler's maxmin utility model), see supplement.

We first explored choices under risk, investigating how the amount of damage to the lPFC, mPFC, and amygdala within the ROIs impacted decisions to gamble. Controlling for overall brain damage, we found that the extent of damage to the lPFC had a pronounced and unique influence on how readily gambles are taken under risk: The greater the damage, the more gambles taken (Table 3, Figure 2A; which was also confirmed with our model-based analysis, Figure S5). We observed no relationship between the amount of damage to the mPFC or amygdala and risky decisions to gamble (Table 3). During ambiguous uncertainty, we observed a similar pattern. Whereas there was no effect of damage to the mPFC or amygdala on willingness to gamble, the more the damage to the lPFC, the more biased an individual was toward taking the gamble (Table 4, Figure 2B; a comparison with the model-based approach revealed inconsistencies, however: see supplement, Figure S5). These findings reveal that patients with lesions to the lPFC exhibit a more global

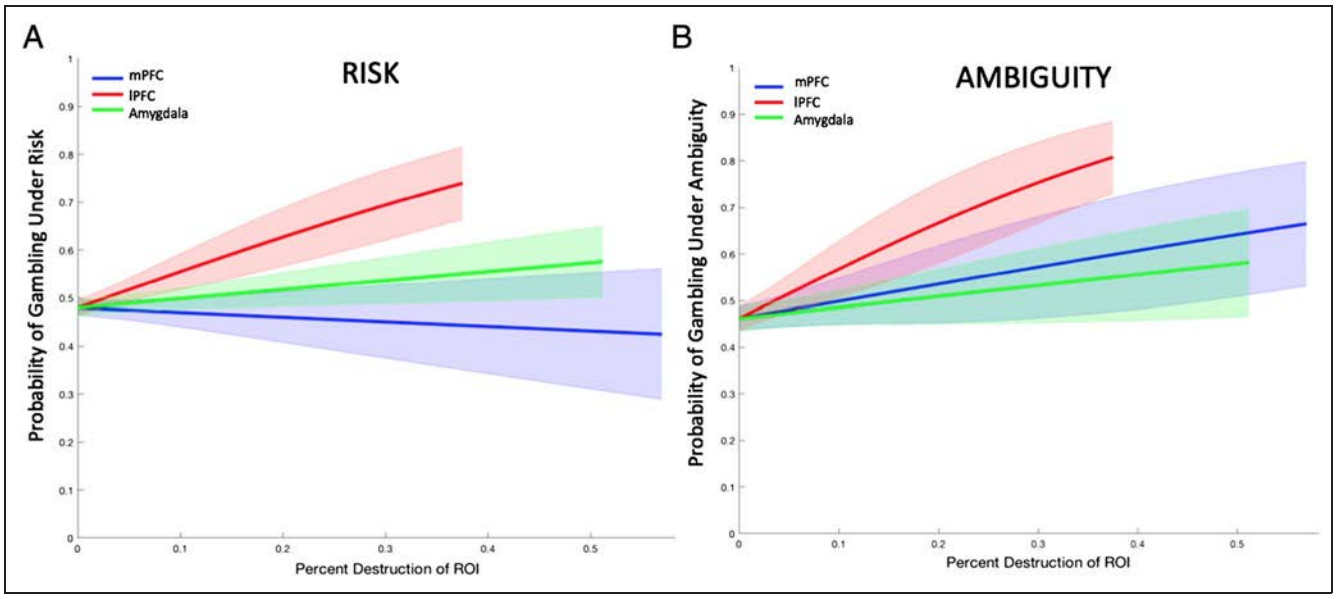

Figure 2. Gambling under risk and ambiguity as a function of lesion group. (A) Gambles under risk. Greater damage to the lPFC resulted in a significant increase in taking risky gambles; there was no relationship between risky gambling and damage to the mPFC or amygdala. (B) Gambles under ambiguity. A similar pattern emerged for decisions made under ambiguity. Error bars reflect 1 *SEM*.

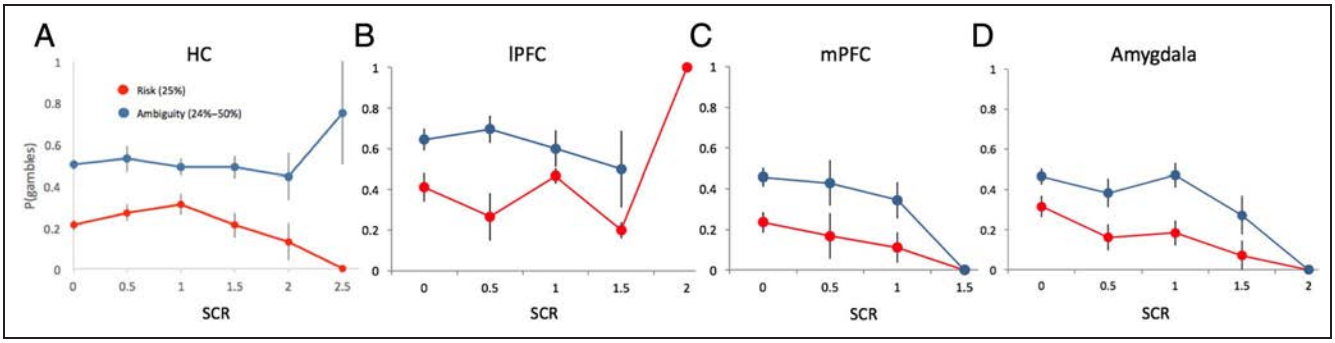

Figure 3. (A) HCs: Dovetailing with past research using the same analysis (FeldmanHall et al., 2016), higher arousal predicts reduced gambling during highly risky trials (low odds of winning the lottery, 25% risk), whereas during ambiguous uncertainty, higher arousal results in increased gambling (collapsing 24–50% ambiguity levels). (B) lPFC patients: Higher arousal responses predict increased gambling during highly risky trials. Nota bene: Arousal levels were attenuated under ambiguity. (C, D) mPFC and MTL patients: Like HCs, higher arousal predicted reduced gambling during highly risky trials in both patient groups. Although there appears to be an aberrant relationship between arousal levels and decisions to gamble under ambiguous uncertainty for both the mPFC and MTL groups, these analyses did not reach significance against HCs. In all panels, SCR is plotted in increments of 0.5 for presentation purposes only; however, during analysis, SCR was treated as a continuous variable (Tables 5 and 6 and Tables S2–S9). Error bars reflect 1 *SEM*.

increase in their tolerance for making both risky and ambiguous decisions (Figure 2).

HCs: Choice and the Relationship with Arousal

Before investigating the gambling–arousal relationship in our patient groups, it is necessary to ensure that our HCs exhibited a relationship between gambling and arousal levels consistent with previous research (FeldmanHall et al., 2016). Accordingly, just as we have done in prior work, we modeled the binary choice to gamble or take the safe option as a function of SCR under each type of uncertainty—for each level of risk and ambiguity. As with our prior work, within the risk domain, results reveal that increasing physiological arousal predicts a greater likelihood of taking the safe option only when the trials are very risky (high risk: $\beta = -1.40$, $t = -4.21$, $p < .001$; Table S2, Figure 3A). In contrast, for ambiguous lotteries, increasing arousal predicts a greater likelihood of taking the gamble for both low and medium ambiguity levels (low: $\beta = 0.56$, $t = 2.32$, $p = .02$; medium: $\beta = 0.61$, $t = 2.50$, $p = .01$; Table S3). These results hold even when controlling for the subjective value of the lottery (we used the residuals from $SCR_{i,t} = \beta_0 + \beta_1 SV_{i,t}$ to predict the probability of taking the gamble, which enables us to probe the direct influence of arousal on choice irrespective of the effects of subjective value). This replicates our earlier work (FeldmanHall et al., 2016), suggesting that in the risk domain, arousal helps to signal that one should refrain from gambling when there is ample evidence that the option will likely reap negative outcomes (e.g., only 25% chance of winning); however, in the ambiguity domain, arousal plays a broader role in the representation of value and the facilitation of increased gambling behavior. For all other HC analyses, see supplement.

Patients: Emotional Arousal and Choice under Risky Uncertainty

Given the finding in HCs that arousal plays a role in decisions to take the sure option when the gamble is very

Table 5. Relationship between Choice and SCR for Highly Risky Gambles: All Patient Groups Compared with HCs

Dependent Variable	*Coefficient* (β)	β *Estimate (SE)*	*t Value*	*p Value*
Risky Choice				
	Intercept	−1.2 (0.15)	−7.56	<.001***
	mPFC SCR	−0.007 (0.007)	−0.98	.32
	lPFC SCR	0.02 (0.007)	2.83	.004*
	MTL SCR	−0.95 (0.005)	−0.88	.37

Highly Risky $\text{Choice}_{i,t} = \beta_0 + \beta_1\ \text{SCR}_{i,t}(\text{Lesion Type})_i$. Where Choice is indexed by participant and trial only for the highly risky trials and Lesion Type is an indicator variable, such that HCs serve as the reference group and SCR is indexed by participants and trial only for the highly risky trials.

*$p < .05$.

**$p < .01$.

***$p < .001$.

risky (Figure 3A, Table S2), we wanted to investigate whether there was evidence of a similar relationship in any of the patient groups. Thus, we ran each patient group through the same analysis pipeline as the HCs. Both the mPFC ($\beta = -2.57$, $t = -3.13$, $p = .001$; Figure 3C, Table S6) and MTL ($\beta = -3.17$, $t = -3.11$, $p = .002$; Figure 3D, Table S8) groups exhibited the same intact arousal–choice relationship observed in HCs, indicating that higher arousal predicts attenuated gambling behavior when the gamble is very risky (25% chance of winning). However, we found no intact relationship between arousal and risky choice for the lPFC group (Table S4). In other words, except those with lesions to the lPFC, every other group (HCs, mPFC patients, and MTL patients) demonstrated the same pattern of increasing arousal predicting a greater likelihood of taking the safe option when the lottery was highly risky (it should be noted that both the lPFC and mPFC groups had overall attenuated arousal responses compared with HCs; Figure S3). Second, we wanted to examine whether this relationship between arousal and choice in each patient group was significantly different from the one exhibited by HCs. Using a hierarchal logistic regression, we indexed highly risky choices as a function of trial-by-trial SCRs and lesion type, where HCs served as the reference category. This revealed that, when there was a 25% chance of winning, only the lPFC group's relationship between arousal and choice was significantly different than the one observed in HCs, and in fact, higher arousal in lPFC patients resulted in greater risk taking when there was a low probability of winning—the opposite relationship to that observed in HCs (Table 5, Figure 3B). Taken together with the evidence from the other groups, it may be the case that lPFC patients gamble more because they are unable to interpret amplified arousal as a signal denoting that the gamble is too risky to be taken.

Patients: Emotional Arousal and Choice under Ambiguous Uncertainty

We followed the same logic for exploring choice under ambiguous uncertainty. In HCs, we observed that, when the trial contained low to medium levels of ambiguous uncertainty, higher arousal led to greater gambling behavior (Figure 3A, Table S3). Interrogating the arousal–choice relationship separately for each lesion group revealed that, when the gambles were somewhat ambiguous, those with lPFC damage (all ps $> .38$; Figure 3B, Table S5), mPFC damage (all ps $> .79$; Figure 3C, Table S7), and unilateral amygdala damage (all ps $> .07$; Figure 3D, Table S9) did not exhibit a relationship between enhanced arousal and increased gambling. We then

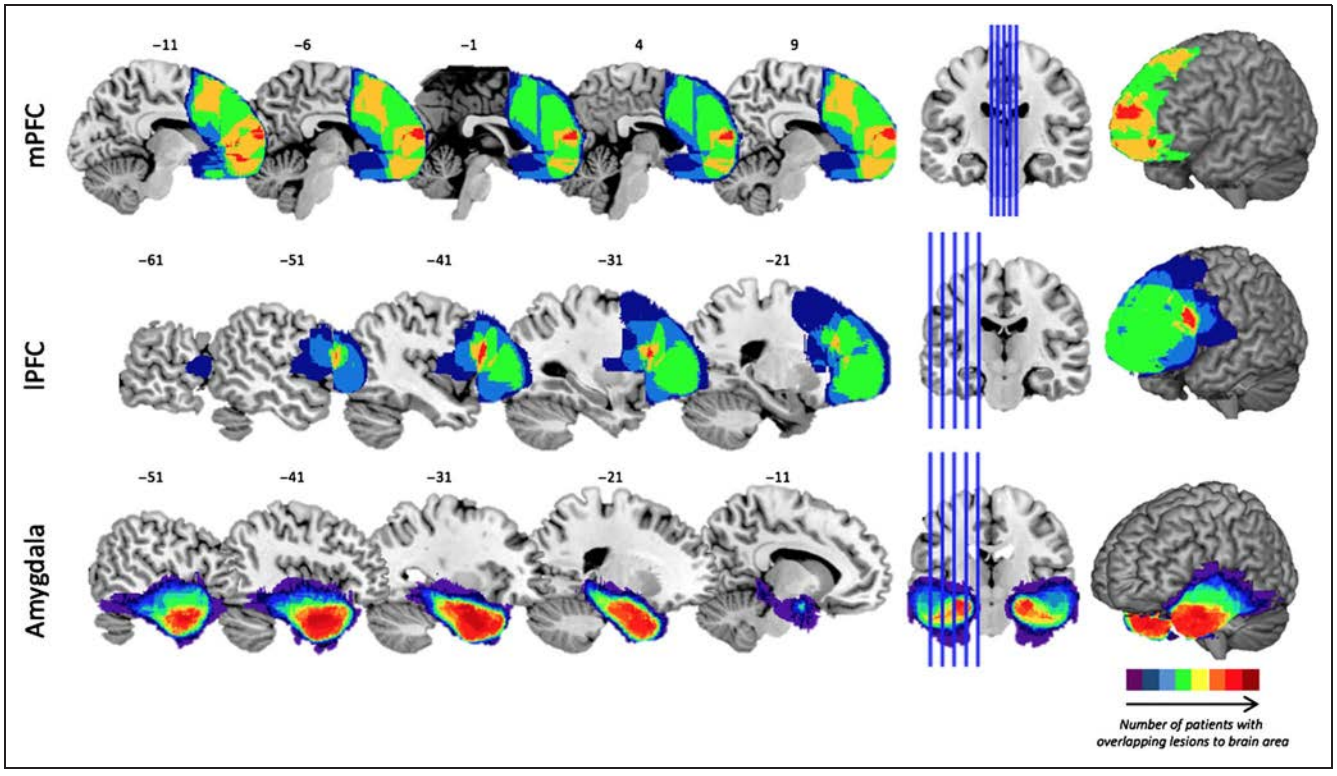

Figure 4. Lesions from patients overlaid on structural MRI slices. Nine patients had lesions to the medial part of the PFC (mPFC), which extended dorsally until the precentral sulcus, with maximum overlap in a region directly rostral to the anterior genu and the anterior pole for six of the nine patients. Eight patients had lesions to the lateral regions of the PFC (lPFC), which extended dorsally until the precentral sulcus and medially until the cingulate, with maximum overlap in seven patients in Brodmann's area 44. Sixteen patients had localized, unilateral lesions to the amygdala, some of which extended posteriorly throughout the hippocampus, but all of which had maximum overlap in the amygdala. Spatial heat maps reflect the number of patients with overlapping lesions to each brain area (see color bar).

Table 6. Relationship between Choice and SCR for Ambiguous Gambles: All Patient Groups Compared with HCs

Dependent Variable	*Coefficient* (β)	β *Estimate (SE)*	*t Value*	*p Value*
Ambiguous Choice				
	Intercept	0.02 (0.11)	−0.33	.76
	mPFC SCR	−0.007 (0.005)	−1.45	.14
	lPFC SCR	0.008 (0.006)	1.50	.13
	MTL SCR	−0.007 (0.004)	−1.40	.17

Ambigous $\text{Choice}_{i,t} = \beta_0 + \beta_1 \text{SCR}_{i,t}(\text{Lesion Type})_i$. Where Choice is indexed by participant and trial and Lesion Type is an indicator variable, such that HCs serve as the reference group and SCR is indexed by participants and trial.

explored whether these seemingly aberrant relationships were statistically different from the one observed in HCs. A hierarchal logistic regression testing the relationship between arousal and choice, as a function of patient group (where the HCs served as the reference category), showed that these differences failed to reach significance between the HCs and the patient groups (Table 6), perhaps because of the overall lower levels of arousal during ambiguous uncertainty observed in all patient groups (e.g., both prefrontal groups failed to generate an SCR response of more than a 1.5 μS).

DISCUSSION

For almost two decades, research investigating decisions under uncertainty have not been able to settle on which regions of the brain are necessary for processing risk and ambiguity. To explore this, we leverage a lesion approach, using both a model-free and model-based procedure to separately estimate individuals' risk and ambiguity attitudes (Tymula et al., 2012; Levy et al., 2010) while simultaneously measuring the body's arousal response (FeldmanHall et al., 2016). First, we replicate our prior work illustrating that the arousal response differentially responds to decisions of risk and ambiguity, such that enhanced arousal is linked either with taking fewer gambles when there is a high probability of loss in a very risky context or with greater exploratory behavior during ambiguous contexts (e.g., increased ambiguity tolerance; FeldmanHall et al., 2016). Second, in contrast to prior work that only showed a relationship between regions of the OFC and amygdala and ambiguity (Hsu et al., 2005), here, we find that the mPFC and amygdala do not appear to be as involved in processing decisions of risk or ambiguity, at least not in our task. In contrast, it appears that the lPFC plays a more general and seemingly necessary role in evaluating all decisions under uncertainty.

More specifically, our findings show that disrupting lPFC function impairs behavior in risky and ambiguous contexts, making individuals more risk and ambiguity seeking across the board. This indicates that the lPFC plays a role in processing uncertainty in a global fashion, likely providing a critical regulatory response that enhances an individual's cautiousness when confronted with decisions of uncertainty. These behavioral patterns were associated with impaired arousal responses: Because lPFC patients did not have an intact arousal response during highly risky lotteries—which would have signaled the risk may not be worth taking—they gambled at disproportionately high rates. In fact, the arousal–choice relationship was in the opposite direction to what was observed in HCs, revealing that higher arousal led to greater gambling behavior when there were very low odds of winning the lottery. This accords with prior work illustrating that the lPFC is critical for flexible regulation of emotional responses (Ochsner, Bunge, Gross, & Gabrieli, 2002) and goal-directed behavior (e.g., emotion regulation; Smittenaar, FitzGerald, Romei, Wright, & Dolan, 2013; Essex, Clinton, Wonderley, & Zald, 2012) and that functional disruption to the lPFC results in a failure to appraise the attendant arousal response. In other words, it may be the case that lPFC patients gamble more because they are unable to interpret arousal as an adaptive signal for how to behave when the choice is uncertain. Accordingly, it appears that, when evaluating risky and ambiguous options, the lPFC is integral in explicitly employing higher-level appraisals that assign value to emotional states and regulatory strategies (Dixon, Thiruchselvam, Todd, & Christoff, 2017), situating it as a unitary hub—or a general system—for evaluating risk and ambiguity.

In contrast, lesions to the mPFC did not influence risky decisions (confirmed with both model-based and model-free analysis). This behavioral pattern dovetails with the arousal results: As with HCs, mPFC patients exhibited normal risk-taking behavior and an intact relationship between higher arousal levels and greater risk aversion when the choice was very risky. There was, however, less consistent evidence of the mPFC and its role in ambiguous uncertainty (revealed by inconsistent results derived by our model-free and model-based approaches). Although we did not find any relationship between the amount of damage to the mPFC and choice using our model-free approach, a model-based approach revealed that those with

functional disruption to the mPFC did exhibit greater ambiguity-seeking behavior (see supplement, Figure S5).[2] Although we are hesitant to draw strong conclusions about the role of the mPFC during ambiguous decision-making given the inconsistency between these two approaches, we further note that the mPFC group also failed to show an intact arousal–choice relationship when the lotteries were ambiguous. Taken in conjunction with the additional impairment in the relationship between arousal and subjective value (see supplement, Table S11), it is possible that the mPFC is involved in contributing critical affective signals that may guide the representation of value during ambiguous choices.

Although these results are modest in nature, a failure to observe intact behavior or an arousal–behavior relationship under ambiguous uncertainty might be reflective of the mPFC's role in evaluating and appraising the value associated with stimuli (Banks, Eddy, Angstadt, Nathan, & Phan, 2007). In the context of our findings, it is possible that the relatively high-level appraisals thought to be carried out by the mPFC may modulate any initial, crude subcortical assessments—which are perhaps supported by engagement of the amygdala. Given that the mPFC is also known to index information about task context (Euston, Gruber, & McNaughton, 2012), other's mental states (Spreng & Grady, 2010; D'Argembeau et al., 2007; Saxe, 2006, Völlm et al., 2006), and value representations associated with discrete stimuli (Levy & Glimcher, 2012; Padoa-Schioppa, 2011; Levy et al., 2010), it would make sense that this region is adept at using environmental clues to guide emotion-related valuations to respond in a more specific, contextualized, and possibly adaptive manner (Ochsner & Gross, 2014). Alternatively, it is possible that the mPFC results are not robust in nature and should thus be treated cautiously.

Finally, the fact that we found no evidence that damage to the amygdala impacted decisions under either risk or ambiguity suggests that there should be restraint in associating the amygdala with decisions of uncertainty. It is worth noting, however, that the MTL group was composed solely of patients with unilateral damage. Although we did not find any observable systematic effects because of the laterality of the lesion, it is quite possible that a group with bilateral damage would exhibit a different pattern of results that may have been masked by the existence of an intact, albeit lateralized, amygdaloid complex.

For the last few decades, the literature has not been able to converge on whether a unified integrated neural system processes both types of uncertainty or whether there are two dissociable systems for processing risk and ambiguity. Here, we find evidence that only one region—the lPFC—seems to be globally necessary for responding appropriately to both risk and ambiguity. This was also reflected by an impaired relationship between arousal and choice. Future work can help further unpack how these uncertainty constructs are processed under different contexts, such as when the uncertainty is especially social in nature.

Acknowledgments

We thank Julian Wills for assistance in data collection.

NYU PROSPEC Collaboration: The New York University Patient Registry for the Study of Perception, Emotion, and Cognition (NYU PROSPEC) includes the following group of clinical researchers and their affiliations.

Karen Blackmon,[1,2] Orrin Devinsky,[1,3,4] Werner K. Doyle,[1] Daniel J. Luciano,[1] Ruben I. Kuzniecky,[1,5] Michael Meager,[6] Siddhartha S. Nadkarni,[1,4] Blanca Vazquez,[1] Soul Najjar,[7,8] Eric Geller,[9] John G. Golfinos,[3,10] Dimitris G. Placantonakis,[3] Daniel Friedman,[1] Jeffrey H. Wisoff,[3,11] Uzma Samadani[3,4,12,13]

[1]Department of Neurology, New York University School of Medicine, New York, NY 10016, USA

[2]Department of Physiology, Neuroscience, and Behavioral Sciences, St. George's University School of Medicine, St. George, Grenada, West Indies

[3]Department of Neurosurgery, New York University School of Medicine, New York, NY 10016, USA

[4]Department of Psychiatry, New York University School of Medicine, New York, NY 10016, USA

[5]Department of Neurology, Hofstra Northwell Health School of Medicine, New York, NY 10075, USA

[6]Department of Psychology, New York University, New York, NY 10003, USA

[7]Lenox Hill Hospital and Staten Island University Hospital, Northwell Health, New York, NY 10075, USA

[8]Department of Neurology, Hofstra North Shore Long Island Jewish School of Medicine, Hempstead, NY 11549, USA

[9]St. Barnabas Medical Center, Livingston, NJ 07039, USA

[10]Department of Otolaryngology-Head and Neck Surgery, New York University School of Medicine, New York, NY 10016, USA

[11]Department of Pediatrics, New York University School of Medicine, New York, NY 10016, USA

[12]Veterans Affairs New York Harbor Health Care System, New York, NY 10010, USA

[13]Department of Physiology & Neuroscience, New York University School of Medicine, New York, NY 10016, USA

Reprint requests should be sent to Oriel FeldmanHall, Department of Cognitive, Linguistic, Psychological Sciences, Carney Institute for Brain Science, Brown University, Providence, RI 02906, or via e-mail: Oriel.feldmanhall@brown.edu.

Notes

1. Supplementary material for this paper can be retrieved from https://static1.squarespace.com/static/56100827e4b0a8aca363cc5f/t/5d2e413a5b6ece00015b155a/1563312442863/RApatient_SI_Final_Press.pdf

2. This may be because, although the Gilboa and Schmeidler model appears to covary fairly accurately with behavior, it may do a less successful job of indexing how ambiguity is represented at the neural level.

REFERENCES

Banks, S. J., Eddy, K. T., Angstadt, M., Nathan, P. J., & Phan, K. L. (2007). Amygdala—Frontal connectivity during emotion regulation. *Social Cognitive and Affective Neuroscience*, *2*, 303–312.

Barr, D. J., Levy, R., Scheepers, C., & Tily, H. J. (2013). Random effects structure for confirmatory hypothesis testing: Keep it maximal. *Journal of Memory and Language*, *68*, 255–278.

Bechara, A. (2004). The role of emotion in decision-making: evidence from neurological patients with orbitofrontal damage. *Brain and Cognition*, *55*, 30–40.

Bechara, A., Damasio, H., & Damasio, A. R. (2000). Emotion, decision making and the orbitofrontal cortex. *Cerebral Cortex*, *10*, 295–307.

Boucsein, W. (1992). *Electrodermal activity*. New York: Plenum Press.

Braithwaite, J. J., & Watson, D. G. (2015). Issues surrounding the normalization and standardisation of skin conductance responses (SCRs). Technical research note. Selective Attention & Awareness Laboratory (SAAL), Behavioural Brain Sciences Centre, School of Psychology, University of Birmingham. https://www.lancaster.ac.uk/media/lancaster-university/content-assets/documents/psychology/ResearchNote_SCRs.pdf.

Brett, M., Anton, J.-L., Valabregue, R., & Poline, J.-B. (2002). Region of interest analysis using the MarsBar toolbox for SPM 99. *Neuroimage*, *16*, S497.

Critchley, H. D., Mathias, C. J., & Dolan, R. J. (2001). Neural activity in the human brain relating to uncertainty and arousal during anticipation. *Neuron*, *29*, 537–545.

D'Argembeau, A., Ruby, P., Collette, F., Degueldre, C., Balteau, E., Luxen, A., et al. (2007). Distinct regions of the medial prefrontal cortex are associated with self-referential processing and perspective taking. *Journal of Cognitive Neuroscience*, *19*, 935–944.

Dawson, M. E., Schell, A. M., & Filion, D. L. (2007). The electrodermal system. In J. T. Cacioppo, L. G. Tassinary, & G. G. Berntson (Eds.), *Handbook of psychophysiology* (pp. 159–181). New York: Cambridge University Press.

Dixon, M. L., Thiruchselvam, R., Todd, R., & Christoff, K. (2017). Emotion and the prefrontal cortex: An integrative review. *Psychological Bulletin*, *143*, 1033–1081.

Ellsberg, D. (1961). Risk, ambiguity, and the savage axioms. *Econometrica*, *29*, 454–455.

Essex, B. G., Clinton, S. A., Wonderley, L. R., & Zald, D. H. (2012). The impact of the posterior parietal and dorsolateral prefrontal cortices on the optimization of long-term versus immediate value. *Journal of Neuroscience*, *32*, 15403–15413.

Euston, D. R., Gruber, A. J., & McNaughton, B. L. (2012). The role of medial prefrontal cortex in memory and decision making. *Neuron*, *76*, 1057–1070.

FeldmanHall, O., Glimcher, P., Baker, A. L., & Phelps, E. A. (2016). Emotion and decision-making under uncertainty: Physiological arousal predicts increased gambling during ambiguity but not risk. *Journal of Experimental Psychology: General*, *145*, 1255–1262.

FeldmanHall, O., Mobbs, D., Evans, D., Hiscox, L., Navrady, L., & Dalgleish, T. (2012). What we say and what we do: The relationship between real and hypothetical moral choices. *Cognition*, *123*, 434–441.

Fischl, B., van der Kouwe, A., Destrieux, C., Halgren, E., Ségonne, F., Salat, D. H., et al. (2004). Automatically parcellating the human cerebral cortex. *Cerebral cortex*, *14*, 11–22.

Gilboa, I., & Schmeidler, D. (1989). Maxmin expected utility with non-unique prior. *Journal of Mathematical Economics*, *18*, 141–153.

Grubb, M. A., Tymula, A., Gilaie-Dotan, S., Glimcher, P. W., & Levy, I. (2016). Neuroanatomy accounts for age-related changes in risk preferences. *Nature Communications*, *7*, 13822.

Holt, C. A., & Laury, S. K. (2002). Risk aversion and incentive effects. *American Economic Review*, *92*, 1644–1655.

Hsu, M., Bhatt, M., Adolphs, R., Tranel, D., & Camerer, C. F. (2005). Neural systems responding to degrees of uncertainty in human decision-making. *Science*, *310*, 1680–1683.

Huettel, S. A., Stowe, C. J., Gordon, E. M., Warner, B. T., & Platt, M. L. (2006). Neural signatures of economic preferences for risk and ambiguity. *Neuron*, *49*, 765–775.

Knight, F. H. (1921). *Risk, uncertainty, and profit*. Boston: Houghton Mifflin Company.

Krain, A. L., Wilson, A. M., Arbuckle, R., Castellanos, F. X., & Milham, M. P. (2006). Distinct neural mechanisms of risk and ambiguity: A meta-analysis of decision-making. *Neuroimage*, *32*, 477–484.

Levy, D. J., & Glimcher, P. W. (2012). The root of all value: A neural common currency for choice. *Current Opinion in Neurobiology*, *22*, 1027–1038.

Levy, I., Snell, J., Nelson, A. J., Rustichini, A., & Glimcher, P. W. (2010). Neural representation of subjective value under risk and ambiguity. *Journal of Neurophysiology*, *103*, 1036–1047.

Ochsner, K. N., Bunge, S. A., Gross, J. J., & Gabrieli, J. D. (2002). Rethinking feelings: An fMRI study of the cognitive regulation of emotion. *Journal of Cognitive Neuroscience*, *14*, 1215–1229.

Ochsner, K. N., & Gross, J. J. (2014). The neural bases of emotion and emotion regulation: A valuation perspective. In J. J. Gross (Ed.), *Handbook of emotional regulation* (pp. 23–41). New York: Guilford.

Padoa-Schioppa, C. (2011). Neurobiology of economic choice: A good-based model. *Annual Review of Neuroscience*, *34*, 333–359.

Saxe, R. (2006). Uniquely human social cognition. *Current Opinion in Neurobiology*, *16*, 235–239.

Smittenaar, P., FitzGerald, T. H., Romei, V., Wright, N. D., & Dolan, R. J. (2013). Disruption of dorsolateral prefrontal cortex decreases model-based in favor of model-free control in humans. *Neuron*, *80*, 914–919.

Spreng, R. N., & Grady, C. L. (2010). Patterns of brain activity supporting autobiographical memory, prospection, and theory of mind, and their relationship to the default mode network. *Journal of Cognitive Neuroscience*, *22*, 1112–1123.

Tymula, A., Rosenberg Belmaker, L. A., Roy, A. K., Ruderman, L., Manson, K., Glimcher, P. W., et al. (2012). Adolescents' risk-taking behavior is driven by tolerance to ambiguity. *Proceedings of the National Academy of Sciences, U.S.A.*, *109*, 17135–17140.

Tymula, A., Rosenberg Belmaker, L. A., Ruderman, L., Glimcher, P. W., & Levy, I. (2013). Like cognitive function, decision making across the life span shows profound age-related changes. *Proceedings of the National Academy of Sciences, U.S.A.*, *110*, 17143–17148.

Völlm, B. A., Taylor, A. N., Richardson, P., Corcoran, R., Stirling, J., McKie, S., et al. (2006). Neuronal correlates of theory of mind and empathy: A functional magnetic resonance imaging study in a nonverbal task. *Neuroimage*, *29*, 90–98.

Wechsler, D., Coalson, D. L., & Raiford, S. E. (2008). *Wechsler Adult Intelligence Scale–Fourth Edition (WAIS-IV)*. San Antonio, TX: Pearson.